Energy Detection and Eigenvalue Based Detection: An Experimental Study Using GNU Radio

Pedro Alvarez*‖, Nuno Pratas *‖, António Rodrigues‖, Neeli Rashmi Prasad*, Ramjee Prasad*
*Center for TeleInFrastruktur
Aalborg University,Denmark
E-mail: {nup,np,prasad}@es.aau.dk
‖Instituto de Telecomunicações/IST, Technical University of Lisbon, Portugal
E-mail: pedro.alvarez@ist.utl.pt, ar@lx.it.pt

***Abstract*—Spectrum sensing plays a key role in enabling the cognitive radios access to vacant spectrum, since it helps avoid interference with the incumbent users. However there are not many studies that show the feasibility of the detectors and analyze their performance under real noise and interference conditions.**

In this work we developed an energy detector to be used on a USRP2 with GNU Radio. We analyzed the detector performance by measuring probabilities of detection and false alarm and how these are influenced by the sensing time and threshold selection. To verify the validity of theoretical expressions comparisons with theoretical values were made.

In this paper we also present an initial study of an eigenvalue detector. It is shown that the filtering done during the decimation of the signal, alters the shape of the noise spectrum and how this consequently degrades the performance of the eigenvalue detector.

I. Introduction

Although spectrum is seen as a scarce natural resource, measurements show that often there are moments in time and space where the spectrum is not being utilized by the services that have allocated it, and therefore is being used inefficiently [1]. To address this issue, regulatory entities are now considering more flexible policies than the traditional fixed frequency allocation [2]. Policies that allow the access of secondary users (SU) to the incumbents or primary users (PU) spectrum, can then improve the spectrum usage efficiency.

Cognitive radio is an emerging technology, which allows dynamic access to unused spectrum. A cognitive radio that has knowledge of the spectrum utilization can opportunistically access it, without causing harmful interference. To achieve this goal, spectrum sensing plays a crucial part in obtaining spectrum knowledge. A variety of techniques for spectrum sensing have been proposed to identify if a channel is occupied or vacant [3].

Energy detection is one of such techniques. It works by measuring the received signal energy and deciding on the presence or absence of the PU, by comparing the received energy level with a threshold. The advantage of this technique is that it does not require knowledge of the transmitted signal by the PU, but it has the disadvantage of requiring an accurate estimation of the received ambient noise power.

Another recently proposed technique is the detection of PU presence by using the eigenvalues of the covariance matrix of the received signal. The motivation of this technique is that due to oversampling, multi path, or multiple receivers, there will be correlation between signal samples [4]. This correlation will be reflected on the eigenvalues of the covariance matrix which can then be used to formulate a detection metric. This technique also does not require knowledge of the transmitted signal characteristics and has the advantage of not requiring an estimation of the noise power [5].

Since cognitive radio is an emerging technology there are not many experimental studies in the literature. The goal of this paper is to present an experimental study of the energy detector and of the eigenvalue detector. Focusing on the energy detector, experimental receiver operating characteristic (ROC) are measured and influence of the sensing times on the probabilities of detection is analyzed. On the eigenvalue detector the existence of some implementation issues are verified. Namely, the effect of the noise not being white is observed in the higher probabilities of false alarm.

This paper is organized as follows: In section II an overview of the energy detection and eigenvalue based detection theoretical models is presented. In section III the experimental setup used is described. In section IV the used algorithms are explained and the experimental results are given, both for the energy and eigenvalue detectors. Finally section V will conclude the paper and present the future work.

II. Theoretical Models

We model the signal detection problem as a hypothesis testing problem, given by:

$$y(t) = \begin{cases} w(t), & H_0 \\ s(t) + w(t), & H_1 \end{cases} \quad (1)$$

where $y(t)$ represents the received signal, $s(t)$ the signal to detect and $w(t)$ additive white Gaussian noise (AWGN). Here the hypothesis H_0 means the absence of signal and H_1 the presence.

The decision on the presence or absence of a signal will be done by evaluating if a certain random variable T, is above or below a certain threshold τ. This variable is defined by the chosen test statistic.

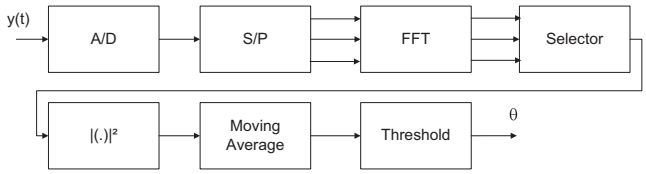

Figure 1: Energy Detection Flow graph

The performance of a detector is evaluated by the probability of false alarm and probability of detection given by equations (2) and (3) respectively.

$$P_F = P\left(T > \tau | H_0\right) \tag{2}$$

$$P_D = P\left(T > \tau | H_1\right) \tag{3}$$

A. Energy Detector

In energy detection in order to evaluate only the energy on the desired bandwidth and to reduce noise power, filtering is necessary. In our experiments the filtering was implemented by applying the fast Fourier transform (FFT) to the signal. This way it is possible to evaluate several sub-channels within a desired bandwidth.

After this the squared magnitude of the FFT bin of interest is computed. The summation of M squared magnitudes is then calculated to obtain an estimate of the signal energy. This value is then compared with a threshold to make a decision on the presence or absence of signal. This is depicted in Figure 1.

The detection metric then becomes:

$$T = \begin{cases} \sum_{m=1}^{M} \left|W\left(m\right)\right|^2, & H_0 \\ \sum_{m=1}^{M} \left|S\left(m\right) + W\left(m\right)\right|^2, & H_1 \end{cases} \tag{4}$$

where $S\left(m\right)$ is considered a deterministic signal, $W\left(m\right)$ is a complex Gaussian random variable whose real and imaginary parts are considered independent and with a variance of σ^2. Then, T will have a χ^2 distribution with $2M$ degrees of freedom under hypotheses H_0, and a non-central χ^2 distribution with $2M$ degrees of freedom, under H_1 [6].

The probability of false alarm is then given by (5) where $\Gamma\left(.,.\right)$ is the upper incomplete Gamma function and $\Gamma\left(.\right)$ is the Gamma function [7]. The probability of detection will be given by (6) where $Q_M(.,.)$ is the generalized Marcum Q function and $\mu = \sum_{m=1}^{M} \left|S\left(m\right)\right|^2$ is the non-centrality parameter of the non central χ^2 distribution [7].

$$P_F = \frac{\Gamma\left(M, \frac{\tau}{2\sigma^2}\right)}{\Gamma\left(M\right)} \tag{5}$$

$$P_D = Q_M\left(\sqrt{\frac{\mu}{\sigma^2}}, \sqrt{\frac{\tau}{\sigma^2}}\right) \tag{6}$$

As we can see by equation (5), to choose a threshold based on the probability of false alarm, an estimate of the noise power is necessary. However an exact estimate of the noise power is impossible due to uncertainty in the measurements and the fact that noise power varies with time. This creates a signal to noise ratio (SNR) wall under which it is impossible to the detect the signal. This limit is given by equation (7) when there are $\pm x$ dB of uncertainty in the noise estimate [8].

$$\gamma_{min} = 10^{\frac{2x}{10}} - 1 \tag{7}$$

B. Eigenvalue Detection

Let $\mathbf{y}(n) = \mathbf{s}(n) + \mathbf{w}(n)$ be a vector of observed samples, where $\mathbf{y}(n)$, $\mathbf{s}(n)$ and $\mathbf{w}(n)$ are given by equations (8) and (9).

$$\begin{aligned} \mathbf{y}(n) &= \left[\begin{array}{cccc} y_1(n) & ... & y_L(n) \end{array}\right]^T \\ \mathbf{s}(n) &= \left[\begin{array}{cccc} s_1(n) & ... & s_L(n) \end{array}\right]^T \\ \mathbf{w}(n) &= \left[\begin{array}{cccc} w_1(n) & ... & x_L(n) \end{array}\right]^T \end{aligned} \tag{8}$$

$$\begin{aligned} y_i(n) &= y((nL + i - 1)T_s) \\ s_i(n) &= s((nL + i - 1)T_s) \\ w_i(n) &= w((nL + i - 1)T_s) \end{aligned} \tag{9}$$

Then the covariance matrix of $\mathbf{y}(n)$, is given by:

$$\mathbf{R_y}(n) = E[\mathbf{y}(n)\mathbf{y}(n)^H] = \begin{cases} \sigma_c^2 \mathbf{I_L}, & H_0 \\ \mathbf{R_s}(n) + \sigma_c^2 \mathbf{I_L}, & H_1 \end{cases} \tag{10}$$

Where $\mathbf{R_s}(n)$ is the covariance matrix of $\mathbf{s}(n)$, $\mathbf{I_L}$ the identity matrix of dimension L and $\sigma_c = E[w(n) * w(n)^*]$.

If there there is correlation between the signal samples, due to oversampling, then $\mathbf{R_s}(n)$ will be different from the identity.

Then the maximum and minimum eigenvalues of covariance matrix will be given by (11),

$$(\lambda_{max}, \lambda_{min}) = \begin{cases} (\sigma_n^2, \sigma_n^2), & H_0 \\ (\rho_{max}(n) + \sigma_n^2, \rho_{min}(n) + \sigma_n^2), & H_1 \end{cases} \tag{11}$$

where $\rho_{max}(n)$ and $\rho_{min}(n)$ are respectively the maximum and minimum eigenvalues of $\mathbf{R_s}(n)$ [5].

Thus, if there is no signal the ratio of maximum and minimum eigenvalues should be one and in the presence of signal the ratio should be greater than one. A metric for the detection of the signal can be defined as:

$$T = \frac{\lambda_{max}}{\lambda_{min}} \tag{12}$$

In practice the covariance matrix has to be estimated. This can be done using the sample covariance matrix given by:

$$\mathbf{R_y}(n) = \frac{1}{N_s} \sum_{i=0}^{N_s - 1} \mathbf{y}(n-i)\mathbf{y}(n-i)^H \tag{13}$$

To select a threshold based on the probability of false alarm an exact expression is derived in [9]. However due to the

computational complexity of it an approximated expression is also derived in [9].

III. Testbed Description

This experimental work was performed in the Real Network module of the S-Cogito Testbed [10]. This module consists of a software defined radio platform, where the RF front end of the nodes is given by the Universal Software Radio Peripheral 2 (USRP2) and the baseband processing is done on a personal computer (PC).

The PC used on the detector was an AMD Athlon 64 X2 Dual Core processor, running Ubuntu 10.10. The PC used for generating the signal was an Intel Pentium4 CPU 3 GHz processor, running Ubuntu 9.04.

The USRP2 was developed by Ettus Inc. and consist of two main boards, a mother board and a daughter board. The daughter board is the actual RF front-end that can be tunned by software. In our experiments we used the XCVR2450 daughter board that works in the 2.4 and 5 GHz bands.

The motherboard incorporates digital to analog converters (DAC), analog to digital converters (ADC) and a FPGA that does the decimation and interpolation. The DAC and ADC communicate with the FPGA at a sampling frequency of 100 Ms/s. The connection to the host PC is done through a Gigabit Ethernet port.

The baseband processing was done using GNU Radio version 3.3.0, which is an open source software development toolkit for signal processing applications. In the GNU Radio architecture, the signal processing blocks are developed in C++ for best performance. The interconnections of the blocks and other non-critical tasks are developed in Python programing language.

The measurements were made in an indoor environment with the USRP2s at an approximate distance of 10 meters and within line of sight of each other.

The signal transmitted was DQPSK signal, modulated with a pseudo random sequence of bits. The signal was generated with a baseband bandwidth of 33.75 kHz and the transmission filter used was a root raised cosine filter with an excess bandwidth factor $\alpha = 0.35$. A flow graph of the transmitter can be seen on Figure 2.

The transmitting USRP2 interpolation was set to 500 and four samples per symbol were used. The gain of the transmitting USRP2 was varied from 0 to 10 dB and the numerical amplifier multiplies the signal by 0.025, 0.050 and 0.1 to get different SNRs.

When starting a flow graph it is necessary to wait for the RF synthesizer to settle and right samples to propagate trough the pipeline. Therefore in all experiments the first 50 ms of data were discarded.

IV. Experimental Results

A. Energy Detection Methodology & Measurements

To analyze the performance of the detector, the receiver was set with the characteristics depicted in Table I. In order

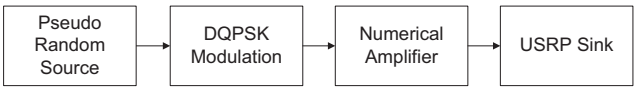

Figure 2: Flow graph of the transmitter

Central Frequency	Sampling Frequency	Gain	FFT Size	FFT Frequency Resolution
5 GHz	12.5 Ms/s	15dB	128	97.656 kHz

Table I: Characteristics of energy detector

to reduce the spectral leakage, a Blackman-Harris window was used in the FFT.

To measure the probabilities of detection and false alarm the flow graph in Figure 3 is used. The following values of M are considered: $M = 100, 200, 500, 1000, 2000$. The decimator keeps one sample in M to eliminate decisions that are correlated. To measure each probability at least 2000 decisions were saved into a file and averaged. Each measurement was repeated 5 times to get a better estimate.

To select thresholds based on the probability of false alarm σ^2 needs to be estimated. With that and the value of M a threshold is obtained using equation (5), having as target a probability of false alarm of 5%.

To estimate the noise in a bin the flow graph in Figure 4 was used. The graph was kept running for 5 seconds generating approximately 480 000 samples that were saved in to a file. The results were then averaged and divided by two to get an estimation of σ^2. This process was repeated 5 times to get a better estimate.

It should be noticed that the USRP2 is not designed as a measuring device. Therefore the measured signals are proportional to the received voltage, but the proportionality constant varies from device to device. This means that to obtain measurements in dBm the device would have to be calibrated. However to perform our experiments this is not necessary and was not done.

To choose a bin to be analyzed, probabilities of false alarm were evaluated in various bins. In Table II we can see the estimated σ^2 on the bins 0 to 5 and the measured probabilities of false alarm with $M = 1000$. One can see that in the lower bins the probabilities are higher then expected. This is explained because the USRP2 with the used FPGA images has a DC offset which increases the probabilities of false alarm. The chosen bin to be analyzed was then the 20th and therefore the transmitter was set to 5.002GHz.

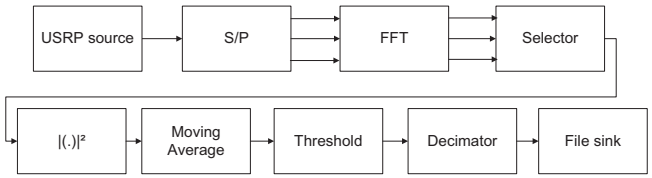

Figure 3: Flow graph to measure probabilities

Bin	0	1	2	3	4	5
$\sigma^2 * 10^6$	1.98	1.84	1.70	1.67	1.66	1.68
Pf	41.5%	25.9%	20.2%	6.8%	7.3%	6.17%

Table II: Measured probabilities of false alarm for various bins

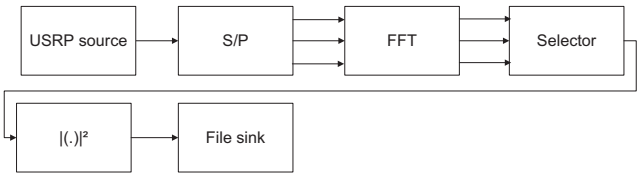

Figure 4: Flow graph to measure noise power

Before measuring probabilities on this bin, σ^2 was estimated and the thresholds for each M computed. The measured probabilities of false alarm can be found in Table III where the threshold was set from $\sigma^2 = 1.67 * 10^{-6}$. One can see they are not far from the theoretical results.

To obtain theoretical results of probabilities of detection, the received power was estimated using the graph in Figure 4. Then μ was estimated by equation (14) where N is the number of samples used to estimate the instantaneous received power.

$$\widehat{\mu} = M * \left(\frac{1}{N} \sum_{m=1}^{N} |S(m) + W(m)|^2 - 2 * \sigma^2 \right) \qquad (14)$$

In Figure 5 we can see the measured probabilities of detection as a function of the averaging time for different values of SNR compared with the theoretical results. The SNR was estimated as $\frac{\widehat{\mu}}{2M\sigma^2}$.

We can see that, even though the channel is not AWGN, the results are not far from the theoretical ones.

To measure the ROC the moving average was fixed at 500, the threshold set from $7.5250 * 10^{-4}$ to $9.1375 * 10^{-4}$ and the transmitted power set in the same manner as before. Using equations (5) and (6) it was possible to obtain the theoretical values of the probabilities for each threshold and each estimated received power.

In Figure 6 we can see the measured and theoretical ROC curves. It is observed a significant error between the two. This probably happens because noise varies with time and errors in the estimation of the received power.

B. Eigenvalue Detection Methodology & Measurements

To compute the eigenvalue ratio of the $\mathbf{R_y}(n)$ the flow chart depicted in Figure 7 was used. Since $\mathbf{R_y}(n)$ is a Hermitian matrix it is only necessary to compute the upper triangular part. In this flow graph we first compute the vector

M	100	200	500	1000	2000
Pf	5.0%	4.7%	5.3%	7.3%	4.1%

Table III: Measured probabilities of false alarm of the energy detector for various averaging times

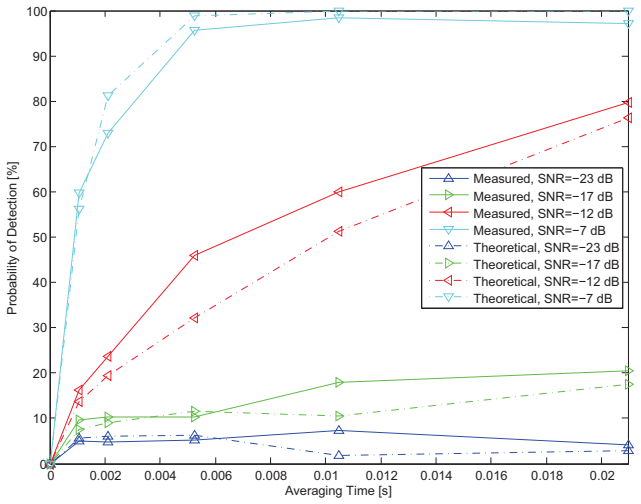

Figure 5: Effect of averaging time in probabilities of detection, using the energy detector

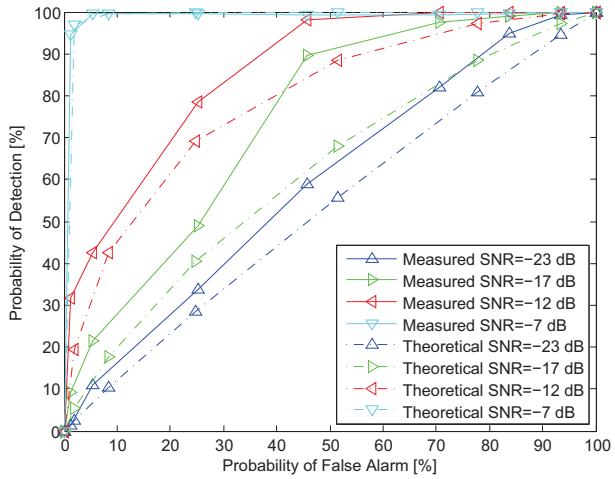

Figure 6: Measured and theoretical ROC of the energy detector

$$v = \left[\; y_1 y_1^* \quad \cdots \quad y_1 y_L \quad y_2 y_2^* \quad y_2 y_3^* \quad \cdots \quad y_L y_L^* \; \right] \qquad (15)$$

This vector is then averaged to obtain the elements that will compose the statistical covariance matrix. In the eigenvalue ratio block the matrix is filled and the eigenvalues computed using the GNU Scientific Library (GSL). To compute the eigenvalues of a hermitian matrix this library uses the symmetric bidiagonalization and QR reduction method. A description of this method can be found in [11].

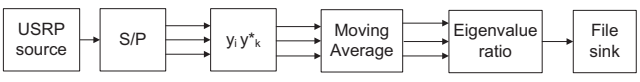

Figure 7: Flowgraph of the eigenvalue detection

M	100	200	500	1000
τ	1.8	1.5	1.3	1.2
Pf	71.5%	79.5%	91.5%	94.8%

Table IV: Measured probabilities of false alarm of the eigenvalue detector for various averaging sizes

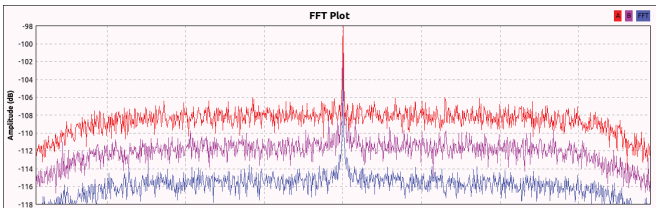

Figure 8: Spectrum in the absence of signal. Red with a decimation of 32, purple 64 and blue 128. All spectra is normalized to the sampling frequency

To measure the performance of the detector a threshold was selected using the approximated expression in [9] with a target probability of false alarm of 5%. A table of the thresholds and measured probabilities of false alarm can be found in Table IV. This table was obtaind using L=3 and a decimation factor of 220.

As shown in Table IV, the measured probabilities of false alarm are far from the theoretical ones. The reason for this is that the observed noise is not white. There are two main reasons for this fact: one is that the signal is filtered to prevent aliasing when it is decimated. This alters the shape of the spectrum, which is no longer flat. The other is that the USRP2 has a DC offset that creates a spike in the spectrum.

Also in Table IV we can see that increasing the sensing time increases the probability of false alarm. This can be explained by the fact that increasing the sensing time increases the sensibility of the detector to the correlation of signals.

In Figure 8 we can see the estimated spectrum at a decimation of 32, 64 and 128, in the absence of a signal. Here we can see at low-frequencies the DC offset and at high frequencies the effect of the filtering. The spectrum was estimated using a 1024 point,rectangular windowed FFT, that was exponentially averaged with $\alpha = 0.055$. All the estimated spectra is normalized to the sampling frequency.

We can see the effect of changing the decimation on the probability of false alarm in Table V. Here we can see that increasing the sampling frequency decreases the probability of false alarm. This can be explained by the fact that increasing the sampling frequency stretches the spectrum making it seem more white.

To see the effect that this has on the performance of the

$Decimation$	32	64	128	256
Pf	34.4%	44.4%	58.2%	66.9%

Table V: Effect of sampling frequency on probabilities of false alarm

M	100	200	500	1000	2000
Pd	3.3%	5.0%	11.3%	19.8%	21.1%

Table VI: Measured probabilities of detection of eigenvalue detector, SNR=-3dB

eigenvalue detector an empirical threshold was selected that would generate a measured probability of false alarm of 5%. The selected decimation was 220, the matrix size $L = 5$ and $M = 100, 200, 500, 1000, 2000$. In Table VI we can see the measured probabilities of detection as a function of the averaging time. The signal was generated like in the subsection IV-A and with an estimated SNR at the receiver of -3 dB.

We can see that the eigenvalue detector is clearly outperformed by the energy detector. This is caused by the necessarily high threshold that was used to diminish the probability of false alarm. This problem can be addressed by compensating the bias, as suggested in [5]

V. Conclusion and Future Work

In this paper an experimental study on energy detection is conducted. We saw that that the theoretical models can be a good approximation of the real phenomena. We have also seen that imperfections of the device can degrade the performance of the detector.

Also an initial study of the eigenvalue detector is conducted. It is seen that imperfections of the hardware and the filtering done by the USRP2 affect the performance of the eigenvalue detector. As a future work, it is necessary to compensate bias of the detector, as is suggested in the appendix A of [5].

References

[1] V. Valenta, R. Maršálek, G. Baudoin, M. Villegas, M. Suarez, and F. Robert, "Survey on spectrum utilization in europe: Measurements, analyses and observations," in *Cognitive Radio Oriented Wireless Networks Communications (CROWNCOM), 2010 Proceedings of the Fifth International Conference on*, June 2010, pp. 1 –5.

[2] FCC, *ET Docket No. 03-322*. Notice of Proposed Rule Making and Order, December 2003.

[3] J. Ma, G. Li, and B. H. Juang, "Signal processing in cognitive radio," *Proceedings of the IEEE*, vol. 97, no. 5, pp. 805 –823, may 2009.

[4] Y. Zeng and Y.-C. Liang, "Spectrum-sensing algorithms for cognitive radio based on statistical covariances," *Vehicular Technology, IEEE Transactions on*, vol. 58, no. 4, pp. 1804 –1815, may 2009.

[5] Y. Zeng and Y. chang Liang, "Eigenvalue-based spectrum sensing algorithms for cognitive radio," *Communications, IEEE Transactions on*, vol. 57, no. 6, pp. 1784 –1793, june 2009.

[6] H. Urkowitz, "Energy detection of unknown deterministic signals," *Proceedings of the IEEE*, vol. 55, no. 4, pp. 523 – 531, april 1967.

[7] J. Proakis, *Digital Communications*, 4th ed. McGraw-Hill, 2001.

[8] A. Sonnenschein and P. Fishman, "Radiometric detection of spread-spectrum signals in noise of uncertain power," *Aerospace and Electronic Systems, IEEE Transactions on*, vol. 28, no. 3, pp. 654 –660, jul 1992.

[9] F. Penna, R. Garello, D. Figlioli, and M. Spirito, "Exact non-asymptotic threshold for eigenvalue-based spectrum sensing," in *Cognitive Radio Oriented Wireless Networks and Communications, 2009. CROWNCOM '09. 4th International Conference on*, june 2009, pp. 1 –5.

[10] N. Pratas, F. Meucci, D. Zrno, N. Prasad, A. Rodrigues, and R. Prasad, "Cogito test-bed - wireless research evolved," in *Cognitive Radio and Advanced Spectrum Management, 2009. CogART 2009. Second International Workshop on*, may 2009, pp. 116 –121.

[11] G. H. Golub and C. F. V. Loan, *Matrix Computations*, 3rd ed. The Johns Hopkins University Press, 1996.